Unusual Photophysical Properties of Substituted Carbazoles

Ravi M. Adhikari and Douglas C. Neckers*

Center for Photochemical Sciences, Bowling Green State University, Bowling Green, Ohio 43403

Received: July 6, 2008; Revised Manuscript Received: October 31, 2008

Photophysical properties of a new class of fluorescent, stable carbazoles (**B1**−**B3**, **G1**−**G3**, and **R1**−**R2**) as a function of excitation wavelength in matrixes and solution are reported. The emission maxima of **B1** and **B3** and **G1**−**G3** show red shifts (6−16 nm) and substantially increased fluorescence quantum yields with a decrease in temperature from 25 to −10 °C. Considerable edge excitation red shift has been observed in **B2**. The emission of **G1** shows both specific and general effects of solvent while intermolecular excitation energy transfer occurs from the naphthyl to the carbazolyl moiety in **G3**. Lippert-Mataga plots confirm the existence of multiple emitting states in each of these compounds.

1. Introduction

Fluorescent organic compounds having large Stoke's shifts have advantages because there can be remarkable light loss due to reabsorption. A major reason for such high Stoke's shift is the formation of intramolecular charge transfer (ICT) states.[1] Edge excitation red shifts (EERS) have been observed in various excited-state reactions leading to photoisomerization,[2] electron transfer,[3] and proton transfer.[4] The application of EERS in viscous and glass-forming fluids,[5] binary solvent mixtures of different polarity proteins,[6] polymers,[7] and micelles has been demonstrated.[4] Studies of luminescence as a function of temperature allow estimation of the activation energy for the deactivation of the excited states.

There have been many studies of carbazole-based compounds in device fabrication[8a−c] but fewer of their photophysical properties in fluids[8d] and polymer matrixes. We have been studying the various photophysical properties of the carbazoles below (Chart 1) in different media including as solids, in solution, and in poly(methyl methacrylate) [PMMA] matrixes.[8a,b]

In this article, we report photophysical properties of the compounds as a function of temperature, concentration, and solvent polarity. The effect of temperature on the emission of carbazoles with substituents in the 3, 6, and 9H positions has been studied to understand the relationship between structure, temperature, and photophysical property. Compounds with both electron-withdrawing (EW) and electron-donating (ED) groups in proper relationship (**R1**) show red-shifted emission in dichloromethane (DCM) and isopropyl alcohol with decreases in temperature, whereas compound **R2** with similar groups of different lengths and geometries of the bridge between the ED group and EW group showed small, but distinct, blue shifts in the same solvents. Studies also were carried out with **R1** and **R2** in different solvents to study the charge transfer (CT) state. Reducing the temperature causes a blue shift in the emission of **B2**.

EERS is observed only when the excitation is at the longer wavelength edge of the lowest energy absorption band. In this article we also report dependence on solvent polarity in the formation of CT on EERS. We observed aggregation quenching in these compounds by carrying out solid-state dilution experiments. Intermolecular energy transfer occurs from the naphthyl moiety to the carbazolyl moiety.

* To whom correspondence should be addressed. E-mail: neckers@photo.bgsu.edu.

2. Experimental Section

2.1. Materials. The synthesis of **B2** is described in the Supporting Information. Syntheses of the remainder of the carbazoles are reported elsewhere.[8b,c] Acetonitrile (ACN), methanol, DCM, pentane, toluene, and hexanes are HPLC grade.

2.2. Measurements. Steady-state absorption and fluorescence spectra were recorded on a Shimadzu UV-2401 spectrophotometer and a Fluorolog-3 spectrometer, respectively. All measurements were carried out at room temperature unless otherwise specified. The quantum yields of fluorescence (Φ_F) in solution were measured following a general method using 9,10-diphenylanthracene ($\Phi_F = 0.9$ in cyclohexane) as the standard.[8a] Sample solutions were taken up in quartz cuvettes and degassed for ∼15 min. The degassed solutions had an absorbance of 0.05−0.09 at the excitation wavelength. The fluorescence spectra of each of the sample solutions were recorded 3−4 times and an average value of integrated areas of fluorescence used for the calculation of Φ_F. The refractive indices of solvents at the sodium D line were used. The Φ_F values in the PMMA were measured following a literature method.[8a] Compounds in dichloromethane were mixed thoroughly with a solution of PMMA in acetonitrile. We cast thin films of the mixture on a quartz plate and allowed the sample to dry. The plate is subsequently inserted into an integrating sphere and the required spectra were recorded.

3. Results and Discussion

3.1. Temperature-Dependent Emission Maxima and Fluorescence Quantum Yields (Φ_F). With a decrease in temperature the emission spectra of **B1**, **B3**, and **G1**−**G3** recorded in DCM show a red-shifted fluorescence emission maxima accompanied by an increase of Φ_F (vide infra). All these nonplanar compounds have significant degrees of free rotation in solution. With decreased temperature, the system attains some solid-state character and molecular packing restricts intramolecular rotation.[9] This explains why Φ_F is also higher at lower temperature. The red-shifted emission spectra (Figures 1, 3, 4, 5, Table 1, and Supporting Information) on decreasing the temperature are in contrast to some literature reports.[1] **B1** shows a red shift of 14 nm in its emission spectra at reduced temperature whereas

10.1021/jp805950v CCC: $40.75
Published on Web 12/19/2008

CHART 1

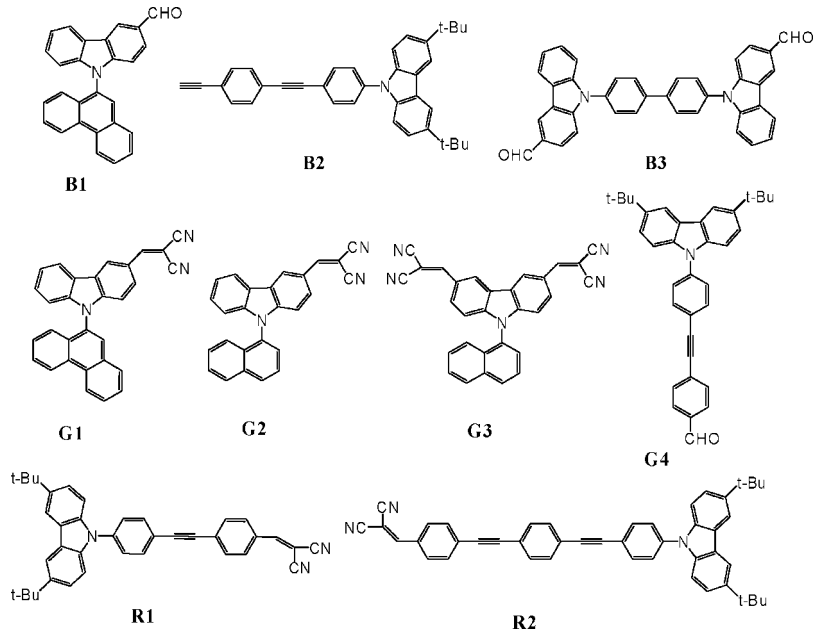

B3 shows red shift only by 6 nm. **B1** is smaller in size and has more freedom of rotation in solution than does **B3**. All these compounds showed positive solvatochromism.[8b]

These compounds possess strong EW and ED groups, thus predicting an intramolecular charge transfer (ICT) state even in the ground state — a state that will be even more stable at reduced temperature. Absorption spectra of these compounds show two bands. The band of higher energy is associated with the S_o-S^1 ($\pi-\pi^*$) transition and that at lower energy is associated with the S_o-ICT* transition.[8b] Since the viscosity of the solvent increases at lower temperature, the reorientational relaxation of the solvent molecules is inhibited, and enhanced stabilization of the ICT* emitting state is expected because reduction of thermal motion allows better alignment of the solute and solvent dipoles. Thus, the ICT excited state dominates over the local excited (LE) state at lower temperature. Consequently, the Franck−Condon excited-state distribution (F-CESD) of the ICT excited state will increase with a decrease in temperature.

When this transition occurs following excitation, two parallel processes occur — excitation to LE and also to ICT*. The F-CESD for ICT* is higher than that for LE (Figure 2), leading to a higher distribution of the ICT* state in the excited-state equilibrium. The dielectric relaxation time of the solvent at lower temperatures might be longer than the fluorescence of both LE and ICT* and thus the solvent relaxation rates from LE−ICT* (k_s) and ICT*−ICTr* (relaxed intramolecular charge transfer excited state) (k_s') also are lower. The fluorescence relaxation rate from ICT* to S_o (k_F) and LE to S_o (k_F') will also be higher than k_s and k_s', respectively. Fluorescence lifetimes of the compounds show biexponential decay; shorter lifetimes are assigned for radiative de-excitation of the ICT* state and longer lifetimes to the de-excitation of the LE state.[8b] Perhaps, the ICT*

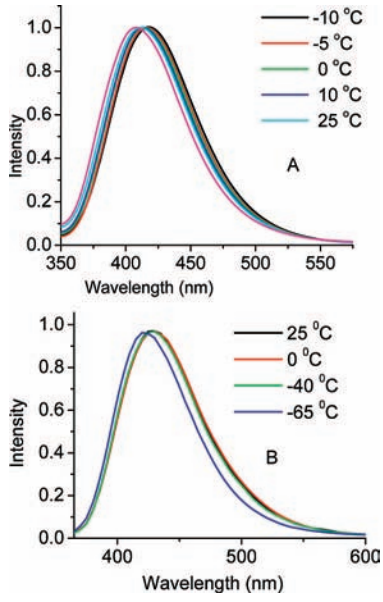

Figure 1. Temperature-dependent emission spectra of (A) **B1**, λ_{ex} = 330 nm recorded in DCM, and (B) **B2**, recorded in isopropyl alcohol, λ_{ex} = 330 nm.

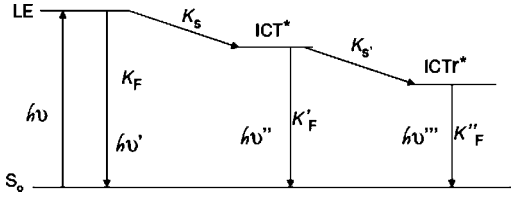

Figure 2. Jablonski diagram showing the possible excitation and de-excitation pathways for **B1**, **B3**, **G1**−**G3**, and **R1**−**R2**.

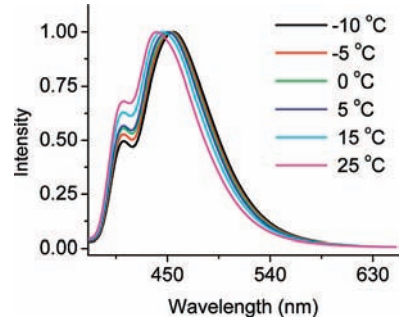

Figure 3. Temperature-dependent emission spectra of **G3** recorded in DCM, λ_{ex} = 370 nm.

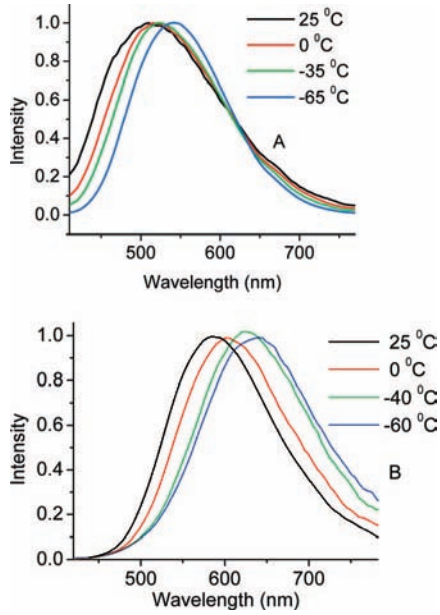

Figure 4. Temperature-dependent emission spectra of **R1** (A) recorded in isopropyl alcohol and (B) recorded in DCM, $\lambda_{ex} = 400$ nm.

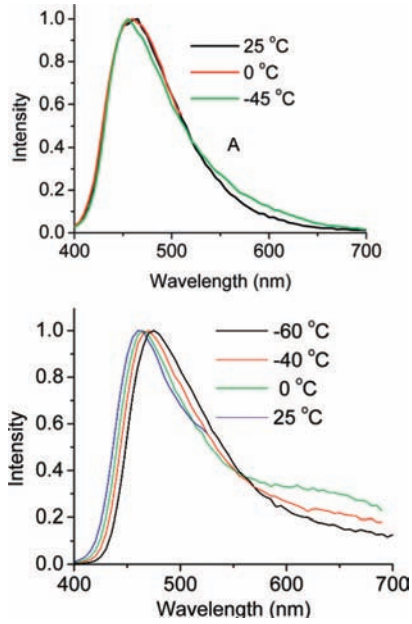

Figure 5. Temperature-dependent emission spectra of **R2** (A) recorded in isopropyl alcohol and (B) recorded in DCM, $\lambda_{ex} = 350$ nm.

contributes the most to the overall fluorescence emission. Lippert-Mataga plots suggest the existence of multiple excited states (vide infra), an effect that increases with the increasingly EW group (**G3** when compared to **G1** and **G2**). These compounds show more red-shifted emission at lower temperature upon excitation at higher energy than that following excitation at lower energy (Table 1).[10]

As in the case of 2-aminophenyl phenylsulfone,[11] **B1** and **B2**, with no strong EW groups, show small blue shifts in emission with a decrease in temperature from 25 to −65 °C (Figure 1B) in isopropyl alcohol.

Remarkable red shifts of as much as 60 nm were observed for **R1** in DCM solution following a reduction in temperature from 25 to −65 °C, Figure 4, where the compound forms a twisted intramolecular charge transfer (TICT) state. Negative solvatochromism[8b] suggested the dipole moment in the excited

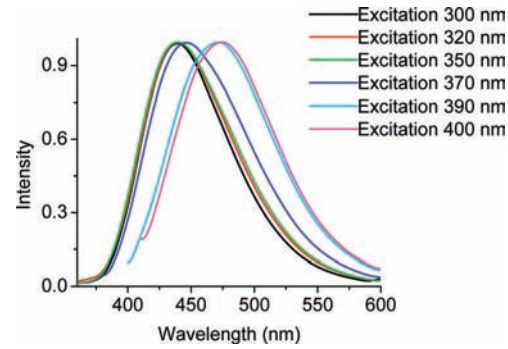

Figure 6. Emission spectra of **B2** recorded in DCM, excitation at different wavelengths.

TABLE 1: Photophysical Data for Compounds B1, B3, G1, G2, and G3 Recorded at Different Temperatures and Different Excitation Wavelengths

		temperature (°C)				
		−10	−5	0	10	25
B1	λ_{max} (nm)	420	416	414	412	406
λ_{ex} 330nm	Φ_F %	10	8	6.2	4.5	3
B3	λ_{max} (nm)	420	418	416	416	414
λ_{ex} 330nm	Φ_F %	10	8.5	7	5.5	3.2
G1	λ_{max} (nm)	422		422	412	408
λ_{ex} 330nm	Φ_F %	12		10	8	6
G1	λ_{max} (nm)	432		434	434	36
λ_{ex} 370 nm	Φ_F %	9		7	5	4
G2	λ_{max} (nm)	390	386	386	382	378
λ_{ex} 330 nm	Φ_F %	21	18	15	12.5	10
G2	λ_{max} (nm)	484	482	482	478	476
λ_{ex} 370 nm	Φ_F %	10	8	7	5	5
G3	λ_{max} (nm)	458	456	456	456	452
λ_{ex} 370 nm	Φ_F %	20	15.5	13	9	7
G3	λ_{max} (nm)	454	454	452	446	440
λ_{ex} 330 nm	Φ_F %	22	18.5	15	13	10

TABLE 2: Photophysical Data for G2 and B2 Recorded in Different Solvents and at Different Excitation Wavelengths

G2	λ_{ex} (nm)	335	355	375	395	405	415	430
DCM	λ_{max} (nm)	382	476	480	481	481	481	488
G2	λ_{ex} (nm)	335	355	375	395	405	415	425
ACN	λ_{max} (nm)	406	496	501	501	504	504	510
B2	λ_{ex} (nm)	300	320	350	370	390	400	
DCM	λ_{max} (nm)	438	438	440	446	473	474	

state is smaller than that in the ground state. Thus, the TICT will be more stabilized in less polar solvents like DCM than in the more polar solvent, isopropyl alcohol. Thus, we observed less red shift (35 nm) for **R1** with a similar reduction in temperature in isopropyl alcohol (Figure 4). **R2** showed a negligible blue shift with a decrease in temperature, Figure 5, where the geometry-optimized ground-state structure shows that the 9H substituted phenylacetylene moiety is not planar.[8b] Conjugation is thus blocked and the compound cannot form a TICT state. The lifetimes of fluorescence of **R2** increase with a decrease in temperature in DCM for the reason explained above. It has been found that on lowering of the temperature, the lifetime increases as a result of the decrease in the nonradiative rate (K_{nr}).[11]

3.2. Excitation Energy Dependence Fluorescence; Edge Excitation Red Shift. In contrast to Kasha's rule we observed that the fluorescence of **G2** and **B2** depends on the excitation energy (Figure 6, Supporting Information, and Table 2). This effect has been referred to as the B shift,[12] the bathochromic luminescence effect,[13] the red-edge effect,[14] and most pertinently EERS[15] or red-edge excitation shift.[16] We observe this remark-

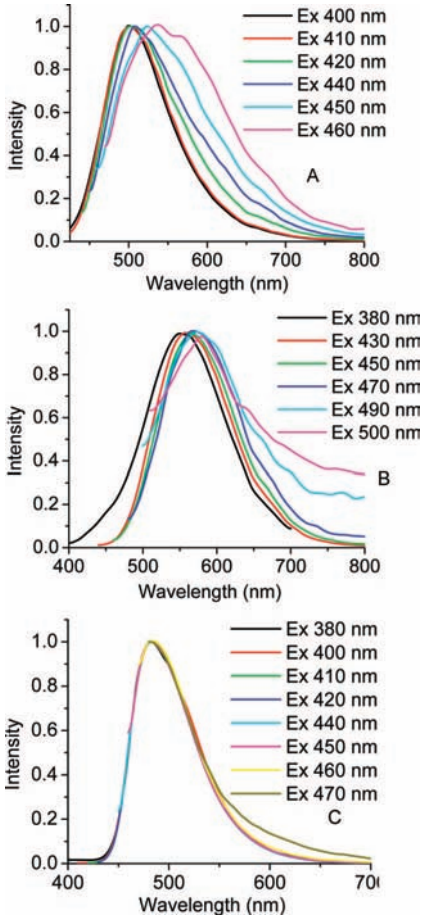

Figure 7. Emission spectra of **R1** recorded in (A) isopropyl alcohol, (B) DCM, and (C) hexanes, excitation at different wavelengths.

able red shift only when excitation is at the longer wavelength edge of the lowest energy absorption band without and serious change in spectral shape. Fletcher[12] described this phenomenon by considering the emission contribution from additional excited species. In a case when the reorientation relaxation time is larger than the fluorescence time, the total fluorescence emission spectrum is a composite of fluorescence emission from differently solvated species governed by F-CESD that is a function of excitation energy.[15]

For a polar compound in polar solvent, the energy required to excite solvated species is a function of solvent orientation. If the excitation energy is smaller, only limited configurations of the ground state may be excited. The excitation with lower energy will excite only the fraction of total fluorophore population which is surrounded by solvent dipoles to decrease the energy of fluorophores. Thus, the resultant total emission lacks some high-energy components and this causes the red-shifted emission.

R1 shifted as much as 34 and 40 nm in DCM and isopropyl alcohol, respectively (Figure 7A and 7B), whereas **G2** shifted 12 and 16 nm in DCM and in ACN, respectively. This is due to the fact that the polar solvents solvate fluorophore more strongly than the nonpolar solvents. Additionally, **R1** forms TICT and **G2** forms ICT so the EERS is more prominent on **R1** than in **G2**. **R1** shows no EERS effect in hexane (Figure 7C), a nonpolar solvent which does not solvate the fluorophore. Mandal et al. explained two requirements for compounds to show EERS behavior; solute−solvent interaction energies leading to inhomogeneity and the excited-state relaxation of the fluorescent species must be slower or comparable to the

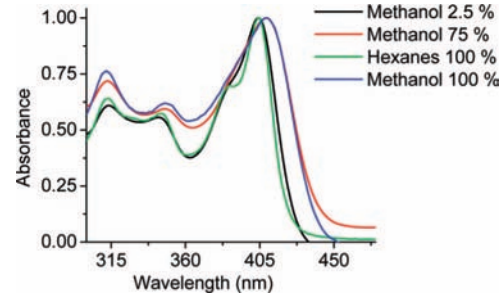

Figure 8. Absorption spectra of **G3** recorded at different hexane: methanol ratios.

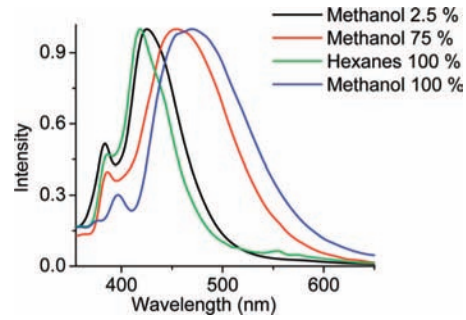

Figure 9. Emission spectra of **G3** recorded in different ratios of hexane to methanol, excited at A_{max}.

fluorescent lifetime of the species.[4] All these compounds appear to meet both requirements. As Lakowicz and Nakamato have reported,[6] the emission spectra shifted little on excitation of these fluorophores at the major absorption band.

3.3. Specific and General Solvent Effects on Emission. The emission maximum of **G3** shifts from 417 nm in hexane to 468 nm in methanol (Figure 9). We observed no change in the absorption spectra (Figure 8). Though we observed no change in the absorption spectrum (Figure 8), addition of 2.5% methanol to hexane, which does not significantly change the orientation polarizability, results in a shift of the emission maximum as a result of H-bonding to the minor solvent by 9 nm. The data in the table 3 shows a gradual red shift in the emission maxima with the fraction of methanol in hexane. So specific solvent−fluorophore interactions occur only in the excited state whereas general solvent−fluorophore interactions occur both in the ground state and the excited state of this compound.

It is worth noting that the emission spectra are broadened on increasing the fraction of methanol due to emission from both the Franck−Condon state and the relaxed state. A specific spectral shift occurs even at a low concentration of methanol in hexane due to the hydrogen bonding of methanol to the nitrogen of the nitrile group on **G3**.

3.4. Fluorescence Switching with Concentration in PMMA Matrix; Aggregation Quenching. We cast thin films of **G1** from a DCM solution to which PMMA in acetonitrile had been added. We observe a progressive red shift in the fluorescence spectrum with an increase in the concentration of **G1** (Figure 10) and a fluorescence quantum yield enhanced 2.5 times on reducing the concentration of **G1** from 5% to 0.01% in the PMMA matrix (Table 4). The linear decrease of fluorescence quantum yield with increase in the concentration of **G1** indicates that, under these circumstances, the fluorescence is being quenched by aggregation. A linear increase of red shift indicates that the fluorescence can be switched by a change in concentration of **G1** in a PMMA matrix. A total shift of 42 nm is observed from changes in concentration.

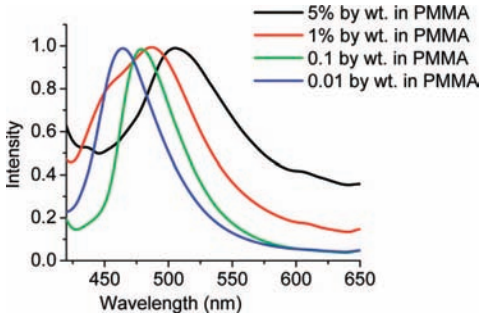

Figure 10. Emission spectra of **G1** recorded in different fractions of **G1** in PMMA matrixes, $\lambda_{ex} = 370$ nm.

TABLE 3: Photophysical Data of G3 Recorded in Different Ratios of Methanol and Hexanes[a]

% of methanol	methanol 2.5%	methanol 75%	methanol 100%	hexanes 100%
λ_{max} (nm)	426	45	468	417

[a] Excitation wavelength = A_{max} for each sample.

TABLE 4: Photophysical Data Recorded for Different Concentrations of G1 in PMMA Matrixes at Different Wavelengths

	% by wt			
	5%	1%	0.1%	0.01%
λ_{ex} 370 nm	1.2	2	5	7
λ_{ex} 330 nm	5	6.2	9	12
λ_{max} at λ_{ex} 370 nm	506	487	477	464

3.5. Intermolecular Energy Transfer. The absorption spectrum of **G3** in DCM shows two distinct bands in the visible (400−430 nm) and UV regions (300−330 nm).[8b] Absorption in the visible region is due to the carbazolyl moiety, whereas that in the UV region is due to the naphthyl group. The sample with $A = 3$ was excited at 315 nm where almost all of the radiation is absorbed by the naphthyl moiety, though the only emission observed is that from the carbazolyl moiety (Figure 11). On excitation of the same sample at 415 nm, we observe similar emission spectra reduced in intensity (Figure 11). If we excite a sample $A = 0.5$ in DCM at 315 nm, we see two emissions: that at 380 nm is residual fluorescence emission from the naphthyl moiety and the other at 460 nm from the carbazolyl group (Supporting Information). This suggests that excitation energy transfer has occurred from the higher energy naphthyl group to the lower energy carbazolyl moiety. Excitation of a sample with a low concentration (absorbance 0.01) at 315 nm shows only one emission band with a maximum intensity at 380 nm (Figure 12).

Again, excitation of the same solution at 415 nm shows an emission with a maximum intensity at 460 nm. This shows

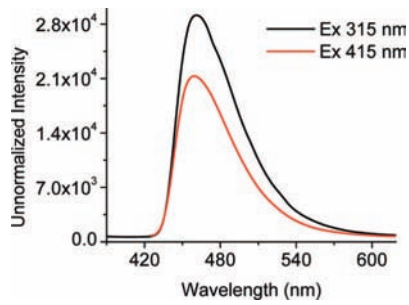

Figure 11. Emission spectra of **G3** recorded in DCM, absorbance of sample = 3.

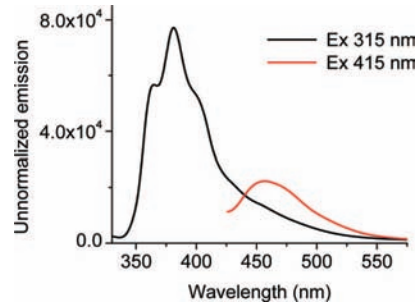

Figure 12. Emission spectra of **G3** recorded in DCM, absorbance of sample = 0.01.

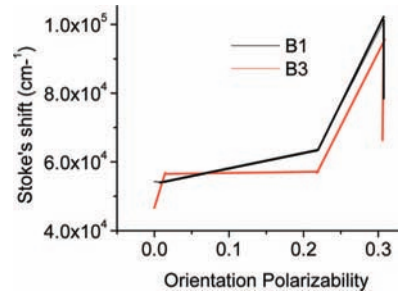

Figure 13. Lippert-Mataga plots for **B1** and **B3** in solvents ACN, methanol, DCM, toluene, and hexanes.

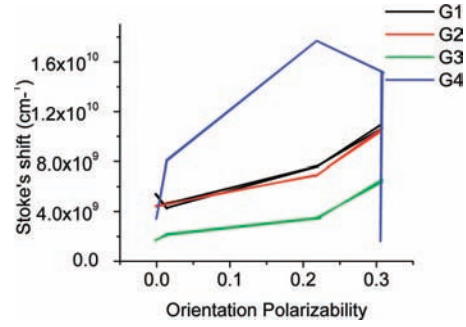

Figure 14. Lippert-Mataga plots for **G1**−**G4** in ACN, methanol, DCM, toluene, and hexane.

there is no excitation energy transfer from the naphthyl moiety to the carbazolyl moiety, proving that the energy transfer must be intermolecular. Additionally, a Gaussian view of the ground-state structure of **G3** shows that the naphthyl moiety is almost orthogonal to the carbazolyl moiety[8b] and, hence, the electronic communication between them is blocked.

3.6. Lippert-Mataga Plot and Its Significance on Specific and General Solvent Effects. The nonlinearity of Lippert-Mataga plots for **B1**−**B2**, **G1-G4**, and **R1-R2** plots (Figures 13−15) indicate the presence of multiple excited states that produce multiple emitting species.[16] Nonlinearity is also evidence for a specific solvent effect on the spectral shift. The possible excited states might be the locally excited state (LE) and/or the ICT* and/or ICTr* states (described above). LE is the emitting species in nonpolar solvents and ICT* and ICTr* are the emitting species in polar solvents. Each of the compounds show multiple emitting species: one locally excited (LE or ^{1}S) and the other ICT, ICTr. **G4**, **R1**, and **R2** probably form twisted intramolecular energy transfer states (TICT) in addition to LE, ICT, and ICTr. TICT formation is possible in the excited state given that the carbazolyl and 9-phenyl moieties are positioned almost orthogonally.[8b]

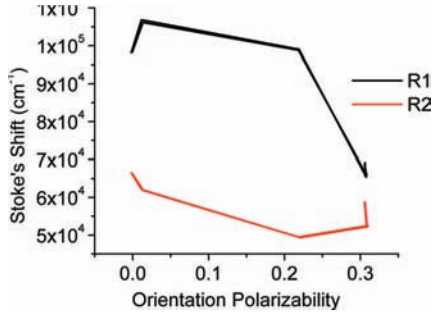

Figure 15. Lippert-Mataga plots for **R1** and **R2** in solvents ACN, methanol, DCM, toluene, and hexanes.

4. Conclusion

Investigation of red-shifted emissions of **B1**, **B3**, and **G1**−**G3** with a decrease in temperature is explained with a Jablonski diagram. F-CESD for ICT* dominates over F-CESD for LE, resulting in the higher contribution from ICT* to the total emission. The extent of EERS is remarkable. Dilution experiments in PMMA matrixes show that aggregation quenching occurs at higher concentrations of the compound. Fluorescence switching to some extent occurs with the change in concentration in PMMA matrixes. Specific solvent effects occur only in the excited state whereas general solvent effects occur both in the ground state and the excited state in these compounds. Lippert-Mataga plots suggest the existence of multiple emitting species. Excitation energy transfer from the naphthyl moiety to the carbazolyl moiety occurs intermolecularly.

Acknowledgment. The paper is Contribution No. 698 from the Center for Photochemical Sciences. We thank Dr. Bipin K. Shah and Dr. Xichen Cai for helpful discussions. This work is supported by the Office of Naval Research.

Supporting Information Available: Emission spectra of **G1** and **G3** at different excitation energies, at different temperatures, and at different concentrations. Synthesis and characterization of **B2**. This material is available free of charge via the Internet at http://pubs.acs.org.

References and Notes

(1) Doroshenko, A. O.; Kyrychenko, A. V.; Waluk, J. *J. Fluoresc.* **2000**, *10*, 41.
(2) Braun, D.; Rettig, W. *Chem. Phys. Lett.* **1997**, *268*, 110.
(3) Demchenko, A. P.; Sytnik, A. S. *J. Phys. Chem.* **1991**, *95*, 10518.
(4) Mandal, P. K.; Paul, A.; Samanta, A. *J. Photochem. Photobiol., A* **2006**, *182*, 113.
(5) Vincent, M.; Galley, J.; Demchenko, A. P. *J. Phys. Chem.* **1995**, *99*, 34931.
(6) Lakowicz, J. R.; Nakamato, S. K. *Biochemistry* **1984**, *23*, 3013.
(7) Al-Hassan, K. A.; El-bayoumi, M. A. *J. Polym. Sci., B* **1987**, *25*, 495.
(8) (a) Adhikari, R. M.; Mondal, R.; Shah, B. K.; Neckers, D. C. *J. Org. Chem.* **2007**, *72*, 4727. (b) Adhikari, R. M.; Shah, B. K.; Neckers, D. C. *J. Org. Chem.* In preparation. (c) Adhikari, R. M.; Shah, B. K.; Neckers, D. C. *Langmuir* Under review. (d) Grabowski, Z. R.; Rotkiewicz, K. *Chem. Rev.* **2003**, *103*, 3899.
(9) Wang, Z.; Shao, H.; Ye, J.; Tang, L.; Lu, P. *J. Phys. Chem. B* **2005**, *109*, 19627.
(10) Viard, M.; Gallay, J.; Vincent, M.; Meyer, O.; Robert, B.; Peternostre, M. *Biophys. Chem.* **1997**, *73*, 2221.
(11) Barigelletti, F. *J. Chem. Soc., Faraday Trans. 2* **1987**, *83*, 1567.
(12) Fletcher, N. *J. Phys. Chem.* **1968**, *72*, 2742.
(13) Rubinov, A. N.; Tomin, V. I. *Opt. Spektrosk.* **1970**, *29*, 1972.
(14) Khalil, O. S.; Selinskar, C. J.; McGlynn, S. P. *J. Chem. Phys.* **1973**, *58*, 1607.
(15) Itoh, K.-I.; Azumi, T. *J. Chem. Phys.* **1975**, *62*, 3431.
(16) Lakowich, J. R. *Principles of Fluorescence Spectroscopy*; Academic/Plenum Publishing: New York, 1999; pp 194−448.

JP805950V